

Cellular stabilization of the melatonin rhythm enzyme induced by nonhydrolyzable phosphonate incorporation

Weiping Zheng¹, Zhongsen Zhang¹, Surajit Ganguly², Joan L Weller², David C Klein² & Philip A Cole¹

Serotonin *N*-acetyltransferase (arylalkylamine *N*-acetyltransferase, AANAT) controls daily changes in the production and circulating levels of melatonin. Here, the significance of the phosphorylation of AANAT was studied using a semisynthetic enzyme in which a nonhydrolyzable phosphoserine/threonine mimetic, phosphonomethylenealanine (Pma), was incorporated at position 31 (AANAT-Pma31). The results of studies in which AANAT-Pma31 and related analogs were injected into cells provide the first direct evidence that Thr31 phosphorylation controls AANAT stability in the context of the intact cells by binding to 14-3-3 protein. These findings establish Thr31 phosphorylation as an essential element in the intracellular regulation of melatonin production. The application of Pma in protein semisynthesis is likely to be broadly useful in the analysis of protein serine/threonine phosphorylation.

Post-translational phosphorylation of tyrosine and serine/threonine residues of proteins plays important roles in regulating protein structure, function and cellular signaling¹. Both 'loss-of-function' and 'gain-of-function' mutants have been used to explore the functional roles played by these phosphorylation events. Commonly used loss-of-function mutations include tyrosine to phenylalanine or serine/threonine to alanine; gain-of-function mutations include the use of aspartate and glutamate as functional surrogates for phosphoserine/phosphothreonine residues. However, success with these replacements has varied^{2–4}. A more physiologically relevant approach is to replace a phosphorylated residue with an irreversible isostere, thereby generating a constitutively phosphorylated protein; resistance to intracellular phosphatases is conferred by the replacement of the bridging oxygen with a methylene group. For example, phosphonomethylenephénylalanine and its difluoro derivative, nonhydrolyzable phosphotyrosine mimetics, have been successfully incorporated into SHP-1 and SHP-2 protein tyrosine phosphatases to study the functional roles of protein tyrosine phosphorylation^{5–7}. These advances point to the possibility that the use of nonhydrolyzable phosphonates might be an informative approach in the analysis of serine/threonine phosphorylation.

We are particularly interested in Thr31 phosphorylation (numbering according to the sheep enzyme) of AANAT, the key enzyme in regulating rhythmic synthesis and secretion of the circadian hormone melatonin^{8,9}. AANAT protein levels rise and fall in a diurnal pattern, driving the nighttime production of melatonin. However, nighttime light exposure in mammals triggers rapid degradation of AANAT and melatonin levels plummet. Cyclic AMP has an important role in regu-

lating AANAT nighttime stability. Furthermore, it has been proposed that Thr31, part of a consensus protein kinase A site located within a binding motif of the 14-3-3 adaptor protein, may be critical in this regard. AANAT has been shown to be phosphorylated *in vivo* on Thr31 and this phosphorylation seems to recruit the 14-3-3 adaptor protein in cells. However, it is not known whether Thr31 phosphorylation and/or 14-3-3 recruitment is directly responsible for inducing AANAT cellular stability (Fig. 1a).

The functional importance of Thr31 phosphorylation in AANAT stabilization in intact cells was studied here using a semisynthetic AANAT wherein Thr31 was replaced by a nonhydrolyzable phosphoserine/phosphothreonine mimetic, phosphonomethylenealanine (Pma) (Fig. 1b). Three other AANATs were also synthesized using a similar approach, in which Thr31 was unchanged or replaced by phosphothreonine or glutamate; these constructs provided controls used for the comparative evaluation of the utility of Pma substitution as an intracellular probe.

The selection of Pma as a substitute for phosphothreonine is consistent with the X-ray structure of the Thr31-phosphorylated AANAT in complex with the 14-3-3 protein (Fig. 1c)¹⁰, which reveals that the bridging oxygen atom of pThr31 is not involved in hydrogen bonding interactions; accordingly, replacement of the bridging oxygen by methylene should not markedly alter the affinity of AANAT for the 14-3-3 protein. The X-ray structure also indicates that each of the nonbridging oxygen atoms of pThr31 makes ionic and hydrogen bonding interactions with side chains from other protein residues; these interactions would also be present in AANAT-Pma31, but not in two alternative mimetics, AANAT-Glu31 and AANAT-Asp31.

¹Department of Pharmacology and Molecular Sciences, Johns Hopkins University School of Medicine, 725 North Wolfe Street, Baltimore, Maryland 21205. ²Section on Neuroendocrinology, Laboratory of Developmental Neurobiology, National Institute of Child Health and Human Development, National Institutes of Health, Bethesda, Maryland 20892. Correspondence should be addressed to P.A.C. (pcole@jhmi.edu).

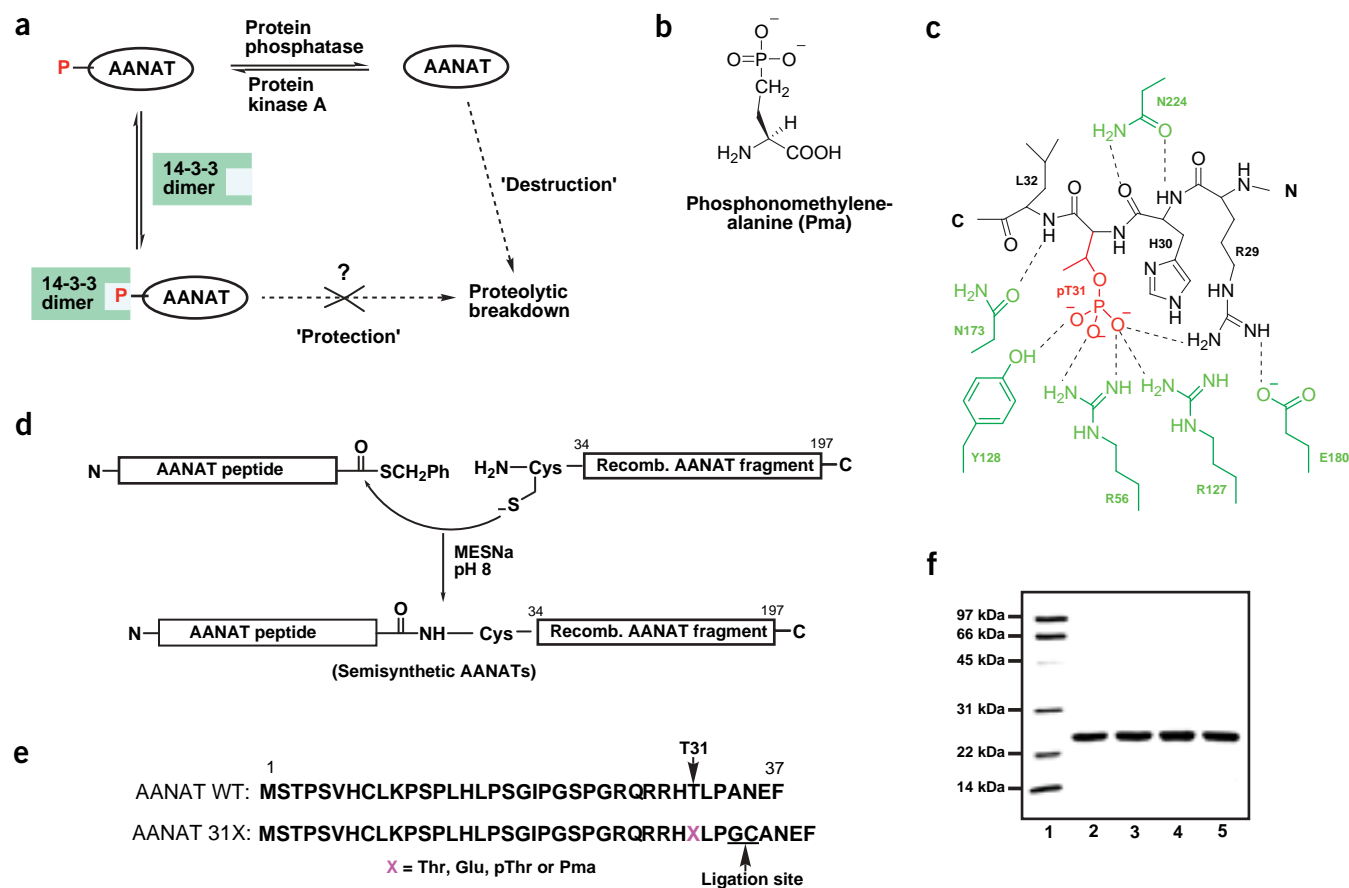


Figure 1 Design, semisynthesis and analysis of AANAT mutants to address the roles of Thr31 phosphorylation in AANAT stabilization *in vivo*. **(a)** Proposed role of phosphorylation and 14-3-3 recruitment in protecting AANAT from proteolytic destruction^{8,9}. **(b)** Chemical structure of phosphonomethyl-L-alanine (Pma). **(c)** Side chain interactions between Thr31-phosphorylated AANAT N terminus and 14-3-3¹⁰. AANAT residues are black except for pT31, which is red. 14-3-3 residues are green. **(d)** Schematic diagram of native chemical ligation¹¹. An AANAT peptide thioester containing the modification of interest interacts with the 1-Cys-containing recombinant AANAT fragment, and after intramolecular rearrangement produces a semisynthetic AANAT with a native amide linkage. MESNa, sodium 2-mercaptoethanesulfonate. **(e)** Partial sequences of wild type (WT) AANAT and semisynthetic AANATs showing the modification (X) and chemical ligation site. **(f)** SDS-PAGE stained with Coomassie blue of purified semisynthetic AANATs. Lane 1, molecular mass markers; lane 2, AANAT-Thr31; lane 3, AANAT-Glu31; lane 4, AANAT-pThr31; lane 5, AANAT-Pma31.

RESULTS

AANAT semisynthesis

The designed semisynthetic AANATs were generated by native chemical ligation of a 1-Cys-containing C-terminal recombinant AANAT fragment with an N-terminal synthetic peptide containing a C-terminal thioester (Fig. 1d)¹¹. The C-terminal recombinant AANAT fragment was produced by engineering a cysteine residue adjacent to a Factor Xa protease cleavage site¹². The peptides containing thioester were synthesized by a modified Fmoc strategy with the C-terminal carboxylic acid derivatized in solution phase followed by side chain deprotection¹³. A glycine residue was added to the C terminus of the peptide sequence to eliminate the epimerization at the C-terminal amino acid and to aid with ligation¹⁴. Overall, the semisynthetic proteins contained an extra Gly-Cys inserted into the protein framework (Fig. 1e). This dipeptide insertion is expected to be well tolerated because the entire AANAT N-terminal segment (residues 1–34) seems to lack a well defined secondary structure and is sensitive to proteolysis¹⁵. Furthermore, this Gly-Cys insertion preserves the 14-3-3 protein-interacting elements². This strategy generated high purity (>90%) products as indicated by SDS-PAGE (Fig. 1f) and MALDI-TOF analyses (data not shown). The specific activities of the semisyn-

thetic AANATs were within two-fold of the wild type (data not shown).

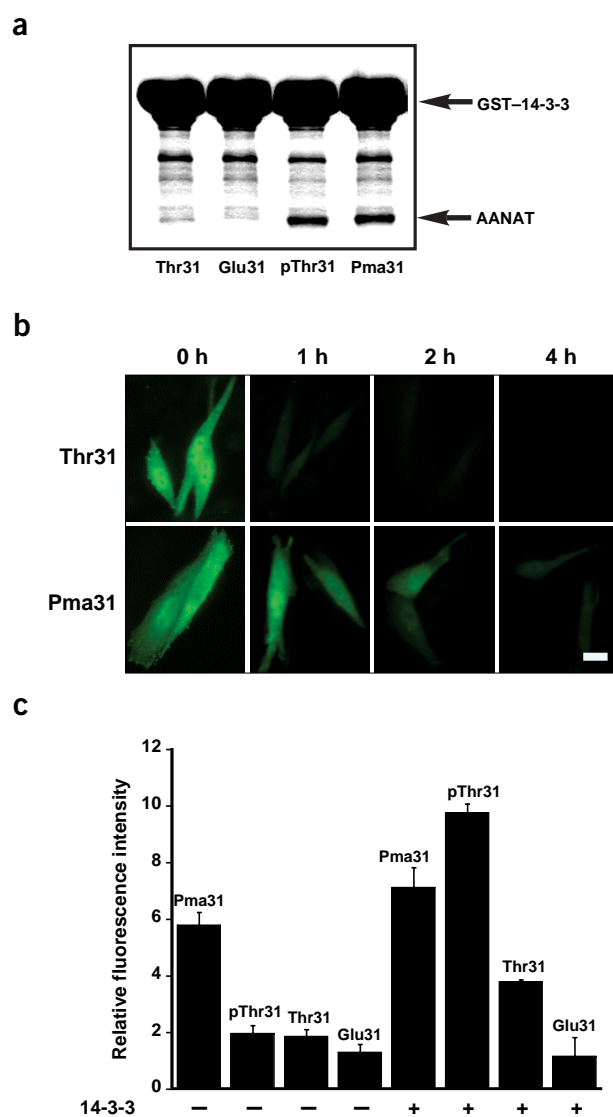
AANAT–14-3-3 protein interaction

The affinity of the semisynthetic AANATs for 14-3-3 protein was examined in an *in vitro* glutathione S-transferase (GST) pull-down assay (Fig. 2a). In this experiment, GST–14-3-3 protein was immobilized on glutathione resin and incubated separately with different semisynthetic AANATs. The quantities of proteins retained on the resin were determined by SDS-PAGE analysis. This assay revealed that the semisynthetic AANAT-Thr31 and AANAT-Glu31 proteins showed minimal binding to 14-3-3 protein, whereas much higher binding was observed for AANAT-pThr31 and AANAT-Pma31. Accordingly, it is evident that in this context pThr31 can be replaced by Pma, but not by glutamate.

Cellular stability of semisynthetic AANATs

To examine whether Thr31 phosphorylation and the subsequent 14-3-3 protein recruitment might be important in maintaining cellular stability of AANAT, each of the semisynthetic proteins was microinjected into the AANAT-null Chinese hamster ovary (CHO)

Figure 2 Evaluation of semisynthetic AANATs *in vitro* and *in vivo*. (a) 14-3-3 interactions with semisynthetic AANATs as assessed by an *in vitro* GST pull-down assay and analyzed by SDS-PAGE stained with Coomassie blue. (b) Degradation of AANAT-Thr31 and AANAT-Pma31 inside CHO cells as reflected by time-dependent decrease in fluorescence intensities. Bar, 20 μ m. (c) Stability of semisynthetic AANATs inside CHO cells under the indicated treatments.



cells¹⁶ and the intracellular levels of the introduced semisynthetic AANATs were measured by immunofluorescence staining with a polyclonal anti-AANAT raised against full-length bacterially expressed ovine AANAT. Fluorescence intensities of semisynthetic AANAT-Pma31 and AANAT-Thr31 were assessed at 0, 1, 2 and 4 h after cellular microinjection (Fig. 2b). After 4 h, AANAT-Pma31 continued to show substantial fluorescence signal, whereas the signal from AANAT-Thr31 was markedly reduced after 1 h. Notably, the observed fluorescence intensity decrease should reflect intracellular AANAT degradation because proteolytic degradation will destroy the epitopes recognized by the polyclonal anti-AANAT. The relative stability of each of the semisynthetic proteins was compared at the 1 h time point. The fluorescence intensity was integrated throughout all positive cells. AANAT-Pma31 showed about a three-fold greater fluorescence intensity as compared with each of the other semisynthetic proteins (Fig. 2c). Taken together, these data indicate that the Pma31 modification confers intracellular stability on AANAT. The greater stability of AANAT-Pma31 compared with AANAT-pThr31 suggests that intracellular phosphatase activity contributes to the mechanism of breakdown of phosphorylated AANAT. This possibility is consistent with the finding that interruption of protein kinase A activation results in the disappearance of AANAT protein, implying that competing phosphatase activity becomes more dominant, and facilitates AANAT degradation¹⁷.

The findings that AANAT-Thr31 and AANAT-Glu31 are less stable (Fig. 2c) and unable to bind tightly with 14-3-3 protein (Fig. 2a), are consistent with the proposal that 14-3-3 protein binding by the phospho- and phosphonoproteins is directly responsible for AANAT stabilization. To further examine this, excess recombinant 14-3-3 protein was co-injected with each of the semisynthetic AANATs. Notably, there seemed to be a marked stabilization of AANAT-pThr31, which had slightly greater stability than AANAT-Pma31, whereas AANAT-Thr31 and AANAT-Glu31 were less affected (Fig. 2c). These observations are consistent with the conclusion that 14-3-3 protein protects or rescues AANAT from degradation within the cell by binding phosphorylated AANAT, thereby preventing dephosphorylation and subsequent degradation.

DISCUSSION

AANAT-Pma31 has been semisynthesized by native chemical ligation¹¹ in an efficient fashion and in quantities that allow for biochemical and cellular studies. The results obtained with the AANAT-Pma31 protein and the three control proteins have provided the first clear and direct evidence for the role of reversible Thr31 phosphorylation in modulating AANAT cellular stability via 14-3-3 interaction. Although it would have been desirable to also examine the stability of the semisynthetic AANATs in cells using traditional western blots or enzyme activity assays, the quantities of protein in the microinjected cells are insufficient to permit these approaches. Fortunately, the anti-AANAT was very effective for these experiments and allowed unambiguous measurements. Moreover, two previous studies further corroborate the protein stability findings reported here. First, it was shown that 14-3-3 protein confers resistance of phosphorylated AANAT protein

to thrombin-mediated proteolysis *in vitro*⁹. Second, western blot evidence indicates that AANAT protein in pineal cells becomes unstable under conditions that suppress protein kinase A-dependent phosphorylation (that is, conditions that favor dephosphorylation and dissociation from 14-3-3)¹⁷. Taken together with these and other previous studies^{8,9,17}, our findings indicate that AANAT's intrinsic cellular instability in unphosphorylated form is the molecular basis for light-induced regulation of melatonin production.

This work shows for the first time that site-specific incorporation of Pma as a nonhydrolyzable phosphoserine/phosphothreonine mimetic is a strategy for dissecting the functional roles and regulatory mechanisms of protein serine/threonine phosphorylations. This should be of general value in future studies on the roles of phosphorylation in regulating protein structure, function and cellular signaling.

METHODS

Peptide thioester synthesis. Based on a published procedure¹³ with our minor modifications, including the use of hexafluoroisopropanol as the weak acid to cleave the fully protected peptide acids from the H-Gly-2CITrt resin, final peptide thioesters were purified (>95%) by reverse-phase HPLC and analyzed by MALDI-TOF to confirm the correct masses. Fmoc-protected amino acids used

were commercially available except for Fmoc-Pma, which was obtained by reacting Fmoc-OSu with commercially available Pma (Tocris Cookson, ~65% pure) and purified by reverse-phase HPLC before use in peptide synthesis.

Cys-AANAT(34–197) generation. The open reading frame was subcloned into the pGEX 6p-1 vector and the GST fusion protein was expressed in *Escherichia coli* and purified as described¹⁸. The GST fusion protein was treated with 10 U Factor Xa per milligram protein at 4 °C for 43 h and the product Cys-AANAT(34–197) was purified as described¹⁹ over the glutathione agarose resin with one extra step over the benzamidine Sepharose resin.

Native chemical ligation and purification of semisynthetic AANATs. These reactions were carried out as described¹¹ with a 10:1 molar ratio of a peptide thioester to Cys-AANAT(34–197) (2.5 mg ml⁻¹) in the presence of 200 mM sodium 2-mercaptoethanesulfonate (MESNa) at 4 °C with gentle mixing for 15 h. The desired product was purified over a CoA-agarose column as described previously¹⁹. All semisynthetic AANATs show high purity (>90%) (SDS-PAGE) and correct molecular mass (±50 Da) (MALDI-TOF). Protein concentrations were determined by the Bradford method.

14-3-3 pull-down assays with semisynthetic AANATs. The general procedures of Lu *et al.*⁷ were followed. An aliquot of 5 µl of GST-14-3-3ζ (2 mg ml⁻¹) immobilized on glutathione agarose resin was incubated with various semisynthetic AANATs (7.4 µl, 1 mg ml⁻¹) and 30 µl of binding buffer (25 mM Tris, pH 7.5, containing 1 mM EDTA and 1 mM DTT) at 16 °C for 4 min. The incubation mixtures were pelleted and the beads were washed three times with the binding buffer at 4 °C and the resulting beads were boiled in 1× SDS-PAGE loading buffer and the supernatants were analyzed by 15% (w/v) SDS-PAGE. This experiment was repeated three times with good reproducibility.

Microinjection experiments. CHO-K1 cells (ATCC) were cultured in ATCC F-12K medium supplemented with 10% (v/v) FBS and 100 U of penicillin-streptomycin, and incubated at 37 °C in the presence of 5% CO₂. The day before the microinjection, cells were seeded onto gridded glass coverslips and grown to 60–70% of confluence. For individual microinjection experiments, semisynthetic AANATs (1.0 mg ml⁻¹, in 45 mM HEPES, pH 7.0, containing 455 mM NaCl, 0.9 mM EDTA, 9 mM DTT, 0.9 mM coenzyme A and 9% (v/v) glycerol) were diluted by three-fold into the following buffer (50 mM Tris, pH 7.5, containing 25 mM NaCl). The same buffer system was also used for the co-injection of semisynthetic AANAT with recombinant 14-3-3ζ (3.0 mg ml⁻¹, prepared as described^{9,10}). After the microinjection at room temperature, cells were maintained at 37 °C in the presence of 5% CO₂ for the indicated time spans before cell fixation and immunofluorescence staining. Cell viability was confirmed by the nuclear staining with DAPI (data not shown). At least 100 cells were injected and two to four independent experiments were carried out for each individual injection or co-injection.

Immunofluorescence staining protocol. Cells were fixed and stained as described⁷ except that primary rabbit antibody (AS 2819) against ovine AANAT(1–205) was used. By using the IPlab software, the fluorescence intensities of all positive cells (visualized above background) were quantified and the sum was normalized by the percentage of injected cells that appeared positive, giving a relative fluorescence intensity value as the indication of the stability of microinjected proteins.

ACKNOWLEDGMENTS

We thank D.B. Murphy and C.J. Janetopoulos for advice on microinjection and immunofluorescence experiments. We are grateful for financial support from the US National Institutes of Health and the Ellison Medical Foundation. Mass spectrometry analysis was carried out in the AB Mass Spectrometry/Proteomics Facility at Johns Hopkins School of Medicine with support from a US National Center for Research Resources shared instrumentation grant, the Johns Hopkins Fund for Medical Discovery and the Institute for Cell Engineering.

COMPETING INTERESTS STATEMENT

The authors declare that they have no competing financial interests.

Received 3 June; accepted 5 September 2003

Published online at <http://www.nature.com/naturestructuralbiology/>

- Hunter, T. Signaling-2000 and beyond. *Cell* **100**, 113–127 (2000).
- Fu, H., Subramanian, R.R. & Masters, S.C. 14-3-3 proteins: structure, function, and regulation. *Annu. Rev. Pharmacol. Toxicol.* **40**, 617–647 (2000).
- Modrof, J. *et al.* Phosphorylation of Marburg virus VP30 at serines 40 and 42 is critical for its interaction with NP inclusions. *Virology* **287**, 171–182 (2001).
- Hao, M. *et al.* Mutation of phosphoserine 389 affects p53 function *in vivo*. *J. Biol. Chem.* **271**, 29380–29385 (1996).
- Lu, W., Shen, K. & Cole, P.A. Chemical dissection of the effects of tyrosine phosphorylation of SHP-2. *Biochemistry* **42**, 5461–5468 (2003).
- Zhang, Z., Shen, K., Lu, W. & Cole, P.A. The role of C-terminal tyrosine phosphorylation in the regulation of SHP-1 explored via expressed protein ligation. *J. Biol. Chem.* **278**, 4668–4674 (2003).
- Lu, W., Gong, D., Bar-Sagi, D. & Cole, P.A. Site-specific incorporation of a phosphotyrosine mimetic reveals a role for tyrosine phosphorylation of SHP-2 in cell signaling. *Mol. Cell* **8**, 759–769 (2001).
- Klein, D.C. *et al.* 14-3-3 proteins in pineal photoneuroendocrine transduction: how many roles? *J. Neuroendocrinol.* **15**, 370–377 (2003).
- Ganguly, S. *et al.* Role of a pineal cAMP-operated arylalkylamine *N*-acetyltransferase/14-3-3-binding switch in melatonin synthesis. *Proc. Natl. Acad. Sci. USA* **98**, 8083–8088 (2001).
- Obsil, T., Ghirlando, R., Klein, D.C., Ganguly, S. & Dyda, F. Crystal structure of the 14-3-3ζ:serotonin *N*-acetyltransferase complex. a role for scaffolding in enzyme regulation. *Cell* **105**, 257–267 (2001).
- Dawson, P.E., Muir, T.W., Clark-Lewis, I. & Kent, S.B. Synthesis of proteins by native chemical ligation. *Science* **266**, 776–779 (1994).
- Erlanson, D.A., Chytil, M. & Verdine, G.L. The leucine zipper domain controls the orientation of AP-1 in the NFATAP-1.DNA complex. *Chem. Biol.* **3**, 981–991 (1996).
- Futaki, S., *et al.* Preparation of peptide thioesters using Fmoc-solid-phase peptide synthesis and its application to the construction of a template-assembled synthetic protein (TASP). *Tetrahedron Lett.* **38**, 6237–6240 (1997).
- Hackeng, T.M., Griffin, J.H. & Dawson, P.E. Protein synthesis by native chemical ligation: expanded scope by using straightforward methodology. *Proc. Natl. Acad. Sci. USA* **96**, 10068–10073 (1999).
- Hickman, A.B., Klein, D.C. & Dyda, F. Melatonin biosynthesis: the structure of serotonin *N*-acetyltransferase at 2.5 Å resolution suggests a catalytic mechanism. *Mol. Cell* **3**, 23–32 (1999).
- Ferry, G. *et al.* Characterization and regulation of a CHO cell line stably expressing human serotonin *N*-acetyltransferase (EC 2.3.1.87). *Cell. Mol. Life Sci.* **59**, 1395–1405 (2002).
- Gastel, J.A., Roseboom, P.H., Rinaldi, P.A., Weller, J.L. & Klein, D.C. Melatonin production: proteasomal proteolysis in serotonin *N*-acetyltransferase regulation. *Science* **279**, 1358–1360 (1998).
- De Angelis, J., Gastel, J.A., Klein, D.C. & Cole, P.A. Kinetic analysis of the catalytic mechanism of serotonin *N*-acetyltransferase (EC 2.3.1.87). *J. Biol. Chem.* **273**, 3045–3050 (1998).
- Khalil, E.M., De Angelis, J., Ishii, M. & Cole, P.A. Mechanism-based inhibition of the melatonin rhythm enzyme: pharmacologic exploitation of active site functional plasticity. *Proc. Natl. Acad. Sci. USA* **96**, 12418–12423 (1999).